Published in final edited form as:

Dev Dyn. 2020 April ; 249(4): 509–522. doi:10.1002/dvdy.134.

Interferon regulatory factor 6 is required for proper wound healing in vivo

Lindsey Rhea[1], **Franklin J. Canady**[2], **Marc Le**[2], **Tanner Reeb**[1,3], **John W. Canady**[4,5], **Deborah S. F. Kacmarynski**[2,4], **Rishika Avvari**[1], **Leah C. Biggs**[2], **Martine Dunnwald**[1,3]

[1]Department of Anatomy and Cell Biology, The University of Iowa, Iowa City, Iowa

[2]Department of Pediatrics, The University of Iowa, Iowa City, Iowa

[3]Interdisciplinary Graduate Program in Genetics, The University of Iowa, Iowa City, Iowa

[4]Department of Otolaryngology, Head and Neck Surgery, The University of Iowa, Iowa City, Iowa

[5]Department of Surgery, The University of Iowa, Iowa City, Iowa

Abstract

Background: Van der Woude syndrome (VWS) is the most common form of syndromic orofacial cleft caused predominantly by mutations in *Interferon Regulatory Factor 6* (*IRF6*). We previously reported that individuals with VWS have increased risk of wound healing complications following cleft repair compared with individuals with nonsyndromic orofacial clefts (nonsyndromic cleft lip and palate—NSCLP). In vitro, absence of IRF6 leads to impaired keratinocyte migration and embryonic wound healing. However, there is currently no data on tissue repair in adult animals and cells with reduced levels of IRF6 like in VWS.

Results: Excisional wounds of $Irf6^{+/-}$ and wild-type animals were analyzed 4 and 7 days post-wounding. Although all wounds were reepithelialized after 7 days, the epidermal and wound volume of repaired wounds was larger in $Irf6^{+/-}$. These data were supported by increased keratinocyte proliferation in the neoformed epidermis and a less mature granulation tissue with increased cytokine levels. This effect was not cell autonomous, as $Irf6^{+/-}$ neonatal keratinocytes in vitro did not exhibit defects in scratch wound closure or proliferation. Keratinocytes from individuals with VWS also migrated similarly to keratinocytes from NSCLP individuals.

Conclusions: These data support a role for IRF6 in wound healing by regulating keratinocyte proliferation, granulation tissue maturation, and cytokine levels.

Keywords

craniofacial; keratinocytes; mouse; Van der Woude syndrome; wound healing

Correspondence: Martine Dunnwald, Department of Anatomy and Cell Biology, The University of Iowa, Iowa City, IA 52245. martine-dunnwald@uiowa.edu.

Lindsey Rhea and Franklin J. Canady contributed equally to this study.

CONFLICT OF INTEREST

The authors state no conflict of interest.

1 | INTRODUCTION

Wound healing is a complex cascade of biological processes that is engaged following injury. Despite years of research, many of the cellular and molecular mechanisms involved in this restorative response remain elusive. In normal conditions, a combination of coordinated cellular proliferation, migration, and differentiation leads to repair of the tissue with minimal sequelae. However, wound healing is often impaired in individuals affected with chronic diseases such as diabetes and cancer, or following large burns.[1,2] Tissue repair complications have also been occasionally observed in genetic disorders.[3] Regardless of the conditions, compromised wound healing is debilitating for the patient and can result in increased infection at the site of injury, hyperproliferation, or scarring.[4]

Interferon regulatory factor (IRF) 6 is a transcription factor that belongs to the larger family of IRFs mediating the interferon response following viral infection.[5] IRF6 is expressed in many cell types including cutaneous and oral keratinocytes,[6,7] innate immune cells,[8] and occasional myocytes and osteocytes.[9,10] IRF6 belongs to a feedback loop with TP63 that regulates epidermal proliferation and differentiation.[11,12] It also contributes to innate immunity by protecting mice from LPS-induced endotoxic shock,[8] and mediating TLR2 and TLR3 signaling in oral and cutaneous keratinocytes, respectively.[13,14] In the absence of *Irf6*, mice exhibit severe cutaneous, limb, and orofacial defects and are perinatal lethal.[6,15] Salivary glands and dental development are also altered in these mice,[16,17] supporting a major role for IRF6 in craniofacial development. In humans, mutations in *IRF6* cause Van der Woude syndrome (VWS, OMIM 119300) and popliteal pterygium syndrome (PPS, OMIM 119500).[18] VWS is an autosomal dominant condition where individuals present with a cleft of their lip and/or palate in addition to pits of their lower lips.[19] Interestingly, our previous retrospective chart study demonstrated that these individuals were more likely to exhibit wound healing complications following surgical repair of their cleft compared with individuals who only had an isolated cleft.[20] Because the cases in our study harbored heterozygous mutations in *IRF6*, it supported our hypothesis that IRF6 plays a role in cutaneous wound healing.

Very little is known about the role of IRF6 in tissue repair. We reported a role for IRF6 in keratinocyte migration and embryonic wound healing.[21] Particularly, murine *Irf6*-knockout keratinocytes were delayed in closing an in vitro scratch compared with wild type cells, and exhibited increased actin stress fibers and active RhoA leading to slower migration.[21] Because *Irf6*-knockout mice are perinatal lethal, we relied on an embryonic wound healing assay to demonstrate that under these ex vivo developmental conditions, IRF6 was required for proper epithelialization. However, no data is currently available on the effect of reduced levels of IRF6 in adult tissue repair in animal models in vivo.

In the current study, we take advantage of $Irf6^{+/-}$ mice as the current best genetic model for VWS (individuals with VWS have only one functional copy of *IRF6*) and evaluate the consequence of decreased levels of Irf6 on adult excisional cutaneous wounds. Our findings show that reduced levels of IRF6 leads to altered tissue repair, and that keratinocytes contributed in a noncell autonomous fashion to this process.

2 | RESULTS

2.1 | Irf6 levels are reduced in Irf6 heterozygous skin and upregulated following wounding

We previously reported the presence of Irf6 in unwounded adult skin and in 1- and 7-day wounds.[21] Here, we extended our previous findings to additional time points and demonstrated the presence of Irf6 in keratinocytes of the migrating tongue and leading edge 4 days post-wounding (Figure 1A). We also observed Irf6 in the granulation tissue (Figure 1A), which we hypothesize are innate immune cells based on our previous findings.[8,21] Seven days post-wounding, Irf6 was restricted to the suprabasal layers of the neoformed epidermis, and occasional cells in the granulation tissue (Figure 1B).

We quantified the level of Irf6 in unwounded and wounded tissues using Western blot. Our data showed a 50% reduction of Irf6 protein levels in adult heterozygous unwounded skin compared with wild-type skin (Figure 1C,D). Following wounding, Irf6 levels increased 2.2- and 3.3-fold in wild-type and heterozygous wounds, respectively, compared to their respective unwounded tissue. These data support our overall hypothesis that Irf6 plays a role in cutaneous wound healing, and that changes in levels of Irf6 could alter tissue repair in vivo.

2.2 | Altered in vivo wound healing in *Irf6*$^{+/-}$ animals

In order to determine whether overall levels of IRF6 alter wound healing in vivo, we performed excisional wounds in *Irf6*$^{+/-}$ and wild-type adult mice. Four days following injury, all the wounds were between 40% and 55% epithelialized with no appreciable difference between groups (Figure 2A,C,I,J). These wounds were fully epithelialized at day 7 (Figure 2B,D,I,J) regardless of the group. However, the *Irf6*$^{+/-}$ animals had significantly increased wound volume and epidermal volume that resulted in a significantly increased percentage of the epidermis in these wounds compared with the wild-type mice (Figure 2E–G). These data suggest that 50 % of Irf6 appears sufficient for epidermal closure of the wound, but yet these wounds presented with altered morphology suggesting an overall dependence of Irf6 for efficient healing.

2.3 | Irf6 is required for the maturation of the granulation tissue

The granulation tissue is the new tissue that forms to replace the injured dermis at the surface of the wound. Characterized by the presence of neoformed blood vessels, deposition of collagen, and temporary presence of myofibroblasts, this provisional tissue allows the keratinocytes to migrate on its surface to close the wound. Following the generation of excisional wounds, wound volume typically decreases, in part because of myofibroblast-dependent contraction and collagen fiber reorganization. The normal decrease in wound volume that occurs as healing progresses continued in both groups at 7 days, with a significantly larger volume in animals with reduced levels of Irf6 (Figure 2E).

To investigate this observation further, we stained with Masson’s Trichrome. This staining allows the visualization of collagen by its turquoise color. Following semiquantitative evaluation (see Material and Methods), our data indicate a lack of collagen deposition 4 days post-wounding in both groups, consistent with the fact that granulation tissue has

not initiated its remodeling at this stage (Figure 3A–C). However, 7 days post-wounding, collagen was present in the granulation tissue of wild type animals and its fibers were organized somewhat parallel to the neoformed epidermis (Figure 3D,D′,G). None of these characteristics were detected in animals with reduced levels of Irf6 at that time point (Figure 3E,E′,G), however, additional turquoise color with parallel collagen fibers was observed in 11-day heterozygous wounds (Figure 3F,F′), suggesting a delayed maturation of the granulation tissue.

The repair of dermal tissue results from an intricate balance between the production of extracellular materials and the activation of fibroblasts into myofibroblasts.[23] We evaluated the expression of α-smooth muscle actin, a marker of myofibroblasts[23,24] and found expression in vascular smooth muscle cells of arterioles in non-wounded healthy tissue flanking the wound (Figure 3H,I). Focusing on 7-day wounds as they demonstrated a difference in collagen organization and trichrome staining (Figure 3D,E), α-smooth muscle actin was detected in occasional cells of the granulation tissue in wild-type animals (Figure 3J). However, we consistently observed a robust expression of α-smooth muscle actin in the granulation tissue of animals with reduced levels of Irf6 (Figure 3K). No myofibroblasts were detected at 4 days in both groups (Figure 3H,I), but some were present in 11-day *Irf6*$^{+/-}$ wounds at the same or slightly elevated levels compared with the wild type at 7 days (Figure 3L). Together, these results suggest that the organization of the collagen fiber network and the presence of α-smooth muscle actin in the granulation tissue are intimately correlated with the level of Irf6, ultimately affecting granulation tissue maturation, which could account for the increased wound volume observed in these samples.

2.4 | Irf6 represses cytokine levels in wounded tissues

As inflammation plays a critical role in cutaneous wound healing,[25] we evaluated the level of cytokines and growth factors in unwounded tissue and 4- and 7-day wounds (Figure 4). As expected, the level of these molecules was low in unwounded samples with no difference between wild type and heterozygotes. Following injury, cytokine and growth factor levels increased 4 days post-wounding (corresponding to the inflammatory phase of tissue repair), and returned to more baseline levels after 7 days. Interestingly, levels of VEGF, IL-1B, IFN-gamma, RANTES, and SDF-1A were all significantly elevated in *Irf6*$^{+/-}$ 4-day wounds compared to wild type (Figure 4A–E). Levels of VEGF and KC were also significantly elevated in *Irf6*$^{+/-}$ 7-day wounds compared to wild type (Figure 4A,F). Of note, IL-6, which we previously showed to be upregulated in a neutrophil-specific *Irf6* conditional knockout,[8] trended like all the other cytokines, however did not reach significance between *Irf6*$^{+/-}$ and wild type (Figure 4G). No statistical difference was observed in GM-CSF (Figure 4H), IL-2 (Figure 4I), and IL 10 (Figure 4J). Globally, these results support a role for Irf6 in repressing the inflammatory response, extending our previously reported findings in endotoxic shock[8] to tissue repair.

2.5 | Reduced Irf6 levels increase epidermal proliferation in neoformed epidermis in vivo

To determine if increased epidermal volume of excisional wounds of *Irf6*$^{+/-}$ mice could be partially attributed to changes in keratinocyte proliferation, immunohistochemistry for proliferating cell nuclear antigen (PCNA) was performed on 4- and 7-day wounds (Figure

5A–C). Although proliferation is typically observed at the wound edge or a short distance from it,[26,27] the proportion of proliferative cells observed in the migrating tongue decreases as the wound heals, as observed in animals of both groups (Figure 5C). In *Irf6*$^{+/-}$, however, our results show persistent proliferation in basal keratinocytes of the neoformed epidermis at day 7 compared with wild-type animals (Figure 5A–C). These data are in support of our morphometric wound analysis showing a larger epidermal volume in this group at this time point (Figure 2F). This effect was specific to the wounded tissue, as the proportion of proliferative basal cells in *Irf6*$^{+/-}$ unwounded epidermis was similar to that of wild-type animals (Figure 5D–F), as was the epidermal thickness (wild type: 12.87 ± 3.7 μm, N = 7, average ± SD; *Irf6*$^{+/-}$: 12.57 ± 2.43 μm, N = 8, average ± SD). This alteration in proliferation did not appear to affect epidermal differentiation, as we did not detect a difference in the pattern of expression of keratin 10 following immunofluorescence of unwounded tissue flanking 7-day wounds (Figure 5G,H).

2.6 | Cell proliferation and migration in vitro is not affected by reduced levels of Irf6

Because we previously reported a role for IRF6 in keratinocyte migration, we asked whether a reduction (and not an absence of, as in our previous studies) in levels of Irf6 would impair keratinocyte proliferation and migration in vitro. To do this, we isolated keratinocytes from *Irf6*$^{+/-}$ and wild-type neonatal epidermis. Morphologically, keratinocytes from both groups were indistinguishable (Figure 6B). Using hypotonic propidium iodine, we assessed the cell cycle status of wild-type and *Irf6*$^{+/-}$ keratinocytes, and did not detect significant changes in the proportion of cells in the different phases of the cell cycle between the two groups (Figure 6A). We also assessed the proliferation rate of basal keratinocytes in embryonic/neonatal epidermis. As observed in adult, we found similar proportion of proliferative cells in wild-type and *Irf6*$^{+/-}$ basal keratinocytes (wild type: 68.87 ± 20.78% PCNA positive in the basal layer, N = 6, average ± SD; *Irf6*$^{+/-}$: 36.08 ± 26.85% PCNA positive in the basal layer, N = 4, average ± SD). Consistent with this observation, the thickness of the epidermis was not significantly different between wild-type and *Irf6*$^{+/-}$ animals (wild type: 53.60 ± 10.5 μm, N = 12, average ± SD; *Irf6*$^{+/-}$: 55.59 ± 14.7 μm, N = 7, average ± SD).

To assess migration, we used a scratch wound assay. Our data show that both wild type and *Irf6*$^{+/-}$ keratinocytes closed the scratch after 24 hours (Figure 6B,C), suggesting that 50% of Irf6 levels in keratinocytes is sufficient for scratch closure in vitro. Together, these data demonstrate that both keratinocyte proliferation in vivo and in vitro, as well as migration in vitro, were not affected by a reduction in Irf6 levels. Globally, with our in vivo wound healing data, our results suggest that the increase in proliferation observed in keratinocytes of the neoformed epidermis of *Irf6*$^{+/-}$ animals is noncell autonomous.

2.7 | Keratinocytes from patients with *IRF6* mutations behaved similarly to cells from patients with NSCLP

To further validate our results obtained with murine cells, we took advantage of a unique collection of keratinocytes isolated from cutaneous biopsies from patients with nonsyndromic cleft lip and palate (NSCLP) or syndromic forms of clefting with *IRF6* mutations (VWS and PPS). We chose samples that were aged- and anatomic site-matched as these two parameters would have the highest impact on keratinocyte behavior.[28,29] As we

previously reported, keratinocytes from both groups were morphologically indistinguishable (Figure 7A).[30] We compared their in vitro behavior following in vitro scratches and found that cells from both groups of individuals showed no difference in scratch closure after 24 hours (Figure 7A,B).

Collectively, these data recapitulate our observations obtained with murine keratinocytes and indicate that in vitro, reduction of IRF6 levels is sufficient for proper migration of keratinocytes.

3 | DISCUSSION

The data presented in this study demonstrate that despite an apparent normal wound healing and complete epithelialization after 7 days, several key aspects of tissue repair were in fact altered in *Irf6*$^{+/-}$ adult mice compared with their wild type counterparts. Particularly, excisional wounds of *Irf6*$^{+/-}$ showed increased epidermal and wound volume compared with wild-type wounds, likely due to an increase in proliferation in the newly formed epidermis and maintenance of myofibroblasts in the granulation tissue. Additionally, inflammatory cytokines and growth factors involved in tissue repair were significantly increased in *Irf6*$^{+/-}$ wounds. Interestingly, neither proliferation nor migration of *Irf6*$^{+/-}$ keratinocytes in vitro was altered, suggesting a noncell autonomous effect.

One of the critical steps of cutaneous wound healing is the migration of keratinocytes to restore the barrier function of the tissue as quickly as possible. A series of cellular processes regulated by several transcription factors and growth factors are involved in keratinocyte migration,[32,33] including IRF6.[21] Our previous work demonstrated that ex vivo in embryos, and in vitro in embryonic keratinocytes, total absence of IRF6 impaired keratinocyte migration.[21] However, data from this study show that partial reduction of IRF6, both in vivo in adult mice and in vitro in embryonic keratinocytes and cells from patients with *IRF6* mutations, is sufficient for functional migration. This leads us to speculate the existence of a threshold level for IRF6, somewhere between 0% and 50%, that is required for proper cell migration. The idea of threshold level has been previously reported for IRF6 in craniofacial development[6,15] and more recently demonstrated for a new function of IRF6 in neurulation.[34] Further studies could take advantage of the unique allelic combinations described in this latter study to define the required IRF6 level for epidermal migration. Among the three syndromic cases with *IRF6* mutations reported in this current study, we determined the genotype of two single nucleotide polymorphisms in *IRF6* that are associated with NSCLP.[35,36] One of the patients had the risk allele at rs2235371 in addition to the presumed disease causing *IRF6* mutation. Cells from this patient did not close the scratch at 24 hours, while the other two did. We recognize this observation is made on a small number of individuals, but it reinforces the potential existence of an IRF6 threshold regulating keratinocyte migration. Although the type of wound healing complications encountered by patients with *IRF6* mutations did not predominantly involve keratinocyte migration (fistula and dehiscence),[20] these results are potentially clinically significant as they would suggest that these individuals can restore their epidermal covering as efficiently as NSCLP or unaffected individuals and that future studies should address other stages of wound healing.

Despite the fact that wounds closed after 7 days, further investigation of *Irf6*$^{+/-}$ adult wounds demonstrated an altered phenotype. Our data showed an increase in the proportion of proliferative basal cells in the migrating tongue and neoformed epidermis, a hallmark of chronic nonhealing ulcers and hypertrophic scars.[37,38] Although all *Irf6*$^{+/-}$ wounds were closed, and the murine model not being ideally suitable to observe hypertrophic scars, these data are in support of a well known previously reported role for IRF6 in regulating keratinocyte proliferation.[6,11,39] Interestingly, this increased rate of proliferation was not observed in *Irf6*$^{+/-}$ unwounded tissue, suggesting that it was unique to the wounded environment and likely non-autonomous in keratinocytes. Follow up studies in *Irf6*$^{+/-}$ cultured keratinocytes did not demonstrate a change in proliferation either. However, these data were obtained in unwounded, confluent keratinocytes under normal culture conditions. Therefore, we cannot rule out the possibility that proliferation may be altered following scratches in vitro. Testing this phenomenon in vitro would potentially be informative, but would remain challenging as the proportion of cells affected by the in vitro wound would be a minimal fraction of the entire cell population, and therefore difficult to detect.

Our data using human keratinocytes from patients with *IRF6* mutations also lead to scratch wound closure, similar to *Irf6*$^{+/-}$ murine cultured keratinocytes. We previously showed that keratinocytes from individuals with VWS had increased proliferative capacity compared to cells from NSCLP individuals, and that in cutaneous hip biopsies, there were twice as many basal keratinocytes proliferating in VWS compared to NSCLP tissues.[30] These data are not consistent with our observation of the *Irf6*$^{+/-}$ murine phenotype. These discrepancies may be due to fundamental differences between murine and human skin, additionally, we do not know the full genetic profile of the patients with *IRF6* mutations or the potential contribution of other genetic variants to the observed change in proliferation.

Reduced levels of Irf6 also had an effect on the wound volume. This parameter is a read out for the maturation of the granulation tissue, the newly formed matrix on which keratinocytes migrate to close the wound. We noticed reduced collagen and high levels of α-smooth muscle actin in *Irf6*$^{+/-}$ mice. This phenotype is reminiscent of what we previously observed in animals with reduced levels of Tgfb3.[22] Tgfb3 is an upstream regulator of Irf6 in oral keratinocytes and palatal epithelium during palatogenesis.[7,40] Results from this study, although not formally tested, support a relationship between these two molecules in cutaneous wounds, similarly to what was observed for craniofacial development, and further validate our overall viewpoint that palatogenesis and cutaneous wounds are “two faces of the same coin”.[41]

The formation of the granulation tissue is dependent on the proper signaling between keratinocytes, innate immune cells, adipocytes, and fibroblasts with the requirement for the migration of collagen-producing fibroblasts to the injured site.[41] Although Irf6 is not detected in fibroblasts, it is expressed in both keratinocytes and innate immune cells, and has been previously reported as a repressor of inflammatory cytokines following endotoxic shock.[8,39] The inflammatory phase of tissue repair is essential to the overall healing process, that must be accompanied by a return to normal levels for completion of the process.[42] Interestingly, the inflammatory phase of the *Irf6*$^{+/-}$ murine wounds was significantly exacerbated and most cytokines had not returned to baseline levels after 7 days. Therefore,

a delay in granulation tissue formation in *Irf6*$^{+/-}$ murine wounds could be due to altered functions of keratinocytes and innate immune cells in their interactions with mesenchymal cells. VEGF, IL-1B, IL-2, IFN-gamma, and to a lesser extend IL-6, could all be mediators of this indirect effect on fibroblasts. Although IRF6 has not traditionally been described as participating in innate immunity like the other IRFs, it has been shown to mediate the Toll-like receptor pathway to regulate cytokines in vitro.[13] Our current data support a role for Irf6 in repressing the inflammatory response of tissue repair, extending our previous findings following endotoxic shock.[8] This is potentially significant in the context of patients with VWS, as they demonstrated an increased risk for dehiscence and fistula following their cleft repair.[20] Dehiscence is often associated with infections,[43] the risk of which one may speculate could be increased in this patient population.

In summary, our studies contribute to our understanding of the function of IRF6 in cutaneous wound healing, ultimately leading to the discovery of additional functions for IRF6 in regulating tissue repair. Moreover, the tissue repair phenotype is added to the list of other malfunctions observed in the heterozygous mouse (ie, brain volume,[44] endotoxic shock response[8]) validating this model as a powerful tool to understand IRF6-related human conditions. As recent reports continue to implicate IRF6 in cancer,[45–47] and the well-established link between chronic wounds and cutaneous carcinogenesis, this model could be a great tool to further investigate this aspect of IRF6 biology.

4 | EXPERIMENTAL PROCEDURES

4.1 | Animals and excisional wounds

All animal procedures were approved by the Animal Care and Use Committee of the University of Iowa. Wild-type and *Irf6* null alleles were maintained on a C57/Bl6N background and previously described.[39] Excisional full thickness wounds were created on the back of the animals using a 6 mm punch biopsy as previously described.[22] Briefly, skin of the scapular region was shaved and two wounds were generated. The removed skin from the punch was preserved and fixed in 4% paraformaldehyde and used as unwounded control tissue. Macroscopic images were acquired immediately following the procedure and later analyzed for their consistent size. Animals were sacrificed 4 and 7 days post-surgery, wounds were harvested and fixed in 4% paraformaldehyde and later embedded in paraffin. Samples were embedded such that the epidermal surface was perpendicular to the blade of the microtome. Serial sectioning was performed throughout the wound, and morphometric analysis performed and computed as previously described using Hematoxylin and Eosin stained sections.[22] Sections in the middle of the wound were also stained with Masson's Trichrome to assess granulation tissue organization. An arbitrary scale system (0 to +++) was used to quantify the amount of collagen (azure blue staining) in the granulation tissue.

4.2 | Western blot analysis and cytokine measurements

Flash frozen punches, 4- and 7-day wounds were ground into powder and protein extracted using radioimmunoprecipitation assay (RIPA) buffer supplemented with protease inhibitor cocktail (Sigma, St. Louis, Missouri; cat# P8340) as previously described.[39] Thirty micrograms of protein were loaded on a 10% Bis-Tris acrylamide gel and transferred

on a PVDF membrane. After blocking the membrane in Tris Buffer Saline with 0.1% Tween 20 (Sigma; cat# P7949) and 10% non-fat dry milk, primary antibodies were incubated overnight at 4°C. Following washes, secondary antibodies were incubated at room temperature for 1 hour. Signal was detected and quantified using the Amersham Imager 600 (GE, Buckinghamshire, UK). Primary antibodies were: anti-rabbit IRF6,[48] anti-mouse GAPDH (Ambion, Austin, Texas; cat#AM4300).

Using the same RIPA extracts, cytokine levels were measured at the Cytokine Core Laboratory (University of Maryland, Baltimore, Maryland) using the Luminex platform.

4.3 | Immunodetection and PCNA quantification

Immunohistochemistry for PCNA (clone PC10, Biomeda, Foster City, California; cat #K110; used at 1/200) was performed according to standard protocol using a diaminobenzidine detection system. Immunofluorescence for alpha smooth muscle actin (Sigma; cat #A_2547; used at 1/400) and keratin 10 (Covance; cat#PRB-159P; used at 1/200) was performed on sections adjacent or near adjacent to the sections stained with Masson's Trichrome using standard protocol. Secondary antibodies were: Biotin-SP-conjugated goat anti-rabbit (Jackson Immunoresearch, West Grove, Pennsylvania; cat #305-065-008; used at 1/200), Alexa Fluor 488 anti-mouse IgG (Invitrogen, Carlsbad, California; cat #A-11017; used at 1/200), and Alexa Fluor 568 anti-rabbit IgG (Invitrogen, Carlsbad, California; cat#A-11011; used at 1/200). Nuclear DNA was labeled with DAPI (4',6-diamidino-2-phenylindole). For PCNA staining, antigen retrieval in citrus buffer was performed, and histochemical detection was performed as previously described.[49] Microscopic observations of histology, Masson's Trichrome staining and PCNA staining were performed with an E600 Eclipse Nikon and photomicrographs recorded with a Nikon DS Ri2 camera. Immunofluorescent images were acquired with a Zeiss 700 Confocal, processed using NIH Image J and presented as maximum projection.

For the quantification of PCNA positive cells in adult and neonatal unwounded murine skin, a total of at least 150 total basal keratinocytes (as defined by their position adjacent to the dermis) per samples were counted over three to four independent images. Percentage of proliferating cells was calculated as the ratio of PCNA positive in the basal layer over the total basal keratinocytes.

For the quantification of PCNA positive cells in wounded samples, total basal keratinocytes were counted in the migrating tongue (see Figure 1A,C, distance between the vertical black lines and the black arrow heads) or neoformed epidermis (see Figure 1B,D, distance between the vertical black lines) and percentage of proliferating cells calculated as described above.

4.4 | Murine keratinocyte culture and cell cycle analysis

Murine keratinocytes were obtained from 1- to 2-day-old animals and cultured in N-medium on collagen IV coated dishes as previously described.[39,50] At about 80% confluency, cells were trypsinized and resuspended in hypotonic propidium iodine as previously described.[51] Briefly, cells were resuspended at 5×10^5 cells/ml in a hypotonic propidium iodide solution (1 mM Tris, 0.1 mM EDTA, 0.1% triton-X100, 3.4 mM Na Citrate, 0.05 mg propidium

iodide). After 15 minutes on ice, the cells were processed through the FACScan (Beckton-Dickinson, San Jose, California) flow cytometer. The DNA content was measured using an 488/635 nm excitation/emission wavelengths and analyzed using the CellQuest software.

4.5 | Scratch wound assay

Scratch wounds were performed on confluent keratinocytes grown in N-medium on collagen IV coated dishes as previously described.[21] Three different areas of the scratch were photographed, analyzed using the ImageJ NIH software, and averaged. Images were acquired 4, 6, 8, 12, and 24 hours following the scratch.

4.6 | Human samples and keratinocyte culture

Human skin tissue from individuals with orofacial cleft was obtained from the skin of the hip during alveolar bone graft, as well as from the skin of the lip during primary cleft lip repair. Samples obtained from the hip were previously reported.[30] Regarding the primary cleft lip repair, the unfused part of the cleft was removed and divided into skin, vermillion, and oral mucosa based on macroscopic evaluation by the surgeon, and always treated separately. Table 1 summarizes the characteristics of the individuals we collected the samples from. A total of nine samples from the hip and three samples from primary cleft lip repair were used in this study.

Keratinocytes from these skin samples were extracted as previously reported.[52] Briefly, samples were rinsed in PBS-1% penicillin streptomycin (Gibco, Waltham, Massachusetts; cat #15140–122) multiple times, cut in thin strips and incubated in Hepes-thermolysin (Sigma, St. Louis, Missouri; cat #9073-78-3) 0.5 mg/ml at 4°C overnight.[53] The following day, the epidermis was mechanically separated from the dermis and isolated in single cell suspension following 30 minutes in trypsin 0.25%-EDTA (Gibco, cat #150050–065) at 37°C. Keratinocytes were grown according to the Rheinwald and Green method using previously irradiated NIH J2 3T3 as feeder layers.[29,52]

ACKNOWLEDGMENTS

We are grateful to Brian Schutte and Jeff Murray for constructive discussions and support along the project. We thank the patients and their families to be willing to donate samples. We thank Kathy Walters from the Central Microscopy Research Facility for technical advice. We also acknowledge the Flow Cytometry Facility, which is a Carver College of Medicine/Holden Comprehensive Cancer Center core research facility at the University of Iowa. The facility is funded through user fees and the generous financial support of the Carver College of Medicine, Holden Comprehensive Cancer Center, and Iowa City Veteran's Administration Medical Center. The cytokine measurements were performed at the University of Maryland School of Medicine Center for Innovative Biomedical Resources Cytokine Core Laboratory—Baltimore, Maryland. This research was supported by funding from NIH/NIAMS to M. D. (AR067739). F. J. C was supported by funding from NIH/NIDCR to Dr. Jeff Murray (DE08559). We appreciate the generous support of Norman and Barbara Johnson through the Paul N. Johnson Professorship of Craniofacial Anomalies to Dr. Kacmarynski.

Funding information

National Institute of Arthritis and Musculoskeletal and Skin Diseases, Grant/Award Number: AR067739; National Institute of Dental and Craniofacial Research, Grant/Award Number: DE08559; Iowa City Veteran's Administration Medical Center; Holden Comprehensive Cancer Center; Carver College of Medicine

REFERENCES

1. Arwert EN, Hoste E, Watt FM. Epithelial stem cells, wound healing and cancer. Nat Rev Cancer. 2012;12:170–180. [PubMed: 22362215]
2. Boyce ST, Glafkides MC, Foreman TJ, Hansbrough JF. Reduced wound contraction after grafting of full-thickness burns with a collagen and chondroitin-6-sullfate (GAG) dermal skin substitute and coverage with biobrane. J Burn Care Rehabil. 1988;9(4):364–370. [PubMed: 3146574]
3. Elsharkawi-Welt K, Hepp J, Scharffetter-Kochanek K. Genetic causes of impaired wound healing. Rare differential diagnosis of the non-healing wound. Hautarzt. 2008;59:893–903. [PubMed: 18936901]
4. Sarrazy V, Billet F, Micallef L, Coulomb B, Desmouliere A. Mechanisms of pathological scarring: role of myofibroblasts and current developments. Wound Repair Regen. 2011;19(Suppl 1): s10–s15. [PubMed: 21793960]
5. Honda K, Taniguchi T. IRFs: master regulators of signalling by toll-like receptors and cytosolic pattern-recognition receptors. Nat Rev Immunol. 2006;6:644–658. [PubMed: 16932750]
6. Ingraham CR, Kinoshita A, Kondo S, et al. Abnormal skin, limb and craniofacial morphogenesis in mice deficient for interferon regulatory factor 6 (*Irf6*). Nat Genet. 2006;38:1335–1340. [PubMed: 17041601]
7. Knight AS, Schutte BC, Jian R, Dixon MJ. Developmental expression analysis of the mouse and chick orthologues of IRF6: the gene mutated in Van der Woude syndrome. Dev Dyn. 2006;235:1441–1447. [PubMed: 16245336]
8. Joly S, Rhea L, Volk P, Moreland JG, Dunnwald M. Interferon regulatory factor 6 has a protective role in the host response to endotoxic shock. PLoS One. 2016;11:e0152385. [PubMed: 27035130]
9. Fakhouri WD, Rhea L, Du T, et al. MCS9.7 enhancer activity is highly, but not completely, associated with expression of Irf6 and p63. Dev Dyn. 2012;241:340–349. [PubMed: 22113860]
10. Thompson J, Mendoza F, Tan E, et al. A cleft lip and palate gene, Irf6, is involved in osteoblast differentiation of craniofacial bone. Dev Dyn. 2019;248:221–232. [PubMed: 30684382]
11. Moretti F, Marinari B, Lo Iacono N, et al. A regulatory feedback loop involving p63 and IRF6 links the pathogenesis of 2 genetically different human ectodermal dysplasias. J Clin Invest. 2010;120:1570–1577. [PubMed: 20424325]
12. Thomason HA, Zhou H, Kouwenhoven EN, et al. Cooperation between the transcription factors p63 and IRF6 is essential to prevent cleft palate in mice. J Clin Invest. 2010;120:1561–1569. [PubMed: 20424327]
13. Kwa MQ, Nguyen T, Huynh J, et al. Interferon regulatory factor 6 differentially regulates toll-like receptor 2-dependent chemokine gene expression in epithelial cells. J Biol Chem. 2014; 289:19758–19768. [PubMed: 24872416]
14. Ramnath D, Tunny K, Hohenhaus DM, et al. TLR3 drives IRF6-dependent IL-23p19 expression and p19/EBI3 heterodimer formation in keratinocytes. Immunol Cell Biol. 2015;93:771–779. [PubMed: 26303210]
15. Richardson RJ, Dixon J, Malhotra S, et al. Irf6 is a key determinant of the keratinocyte proliferation-differentiation switch. Nat Genet. 2006;38:1329–1334. [PubMed: 17041603]
16. Chu EY, Tamasas B, Fong H, et al. Full spectrum of postnatal tooth phenotypes in a novel Irf6 cleft lip model. J Dent Res. 2016;95:1265–1273. [PubMed: 27369589]
17. Metwalli KA, Do MA, Nguyen K, et al. Interferon regulatory factor 6 is necessary for salivary glands and pancreas development. J Dent Res. 2018;97:226–236. [PubMed: 28898113]
18. Kondo S, Schutte BC, Richardson RJ, et al. Mutations in IRF6 cause Van der Woude and popliteal pterygium syndromes. Nat Genet. 2002;32:285–289. [PubMed: 12219090]
19. van der Woude A. Fistula labii inferioris congenita and its association with cleft lip and palate. Am J Hum Genet. 1954;6: 244–256. [PubMed: 13158329]
20. Jones JL, Canady JW, Brookes JT, et al. Wound complications after cleft repair in children with Van der Woude syndrome. J Craniofac Surg. 2010;21:1350–1353. [PubMed: 20856020]
21. Biggs LC, Naridze R, Demali KA, et al. Interferon regulatory factor 6 regulates keratinocyte migration. J Cell Sci. 2014;127:2840–2848. [PubMed: 24777480]

22. Le M, Naridze R, Morrisson J, et al. Transforming growth factor beta 3 is required for proper excisional wound repair in vivo. PLoS One. 2012;7:e48040. [PubMed: 23110169]
23. Hinz B. Formation and function of the myofibroblast during tissue repair. J Invest Dermatol. 2007;127:526–537. [PubMed: 17299435]
24. Reynolds AJ, Chaponnier C, Jahoda CAB, Gabbiani G. A quantitative study of the differential expression of alpha-smooth muscle actin in cell populations of follicular and non-follicular origin. J Invest Dermatol. 1993;101:577–583. [PubMed: 7691972]
25. Brazil JC, Quiros M, Nusrat A, Parkos CA. Innate immune cell-epithelial crosstalk during wound repair. J Clin Invest. 2019;129:2983–2993. [PubMed: 31329162]
26. Aragona M, Dekoninck S, Rulands S, et al. Defining stem cell dynamics and migration during wound healing in mouse skin epidermis. Nat Commun. 2017;8:14684–14698. [PubMed: 28248284]
27. Park S, Gonzalez DG, Guirao B, et al. Tissue-scale coordination of cellular behaviour promotes epidermal wound repair in live mice. Nat Cell Biol. 2017;19:155–163. [PubMed: 28248302]
28. Barrandon Y, Green H. Three clonal types of keratinocyte with different capacities for multiplication. Proc Natl Acad Sci U S A. 1987;84:2302–2306. [PubMed: 2436229]
29. Rheinwald JG, Green H. Serial cultivation of strains of human epidermal keratinocytes: the formation of keratinizing colonies from single cells. Cell. 1975;6:331–343. [PubMed: 1052771]
30. Hixon K, Rhea L, Standley J, Canady FJ, Canady JW, Dunnwald M. Interferon regulatory factor 6 controls proliferation of keratinocytes from children with Van der Woude syndrome. Cleft Palate Craniofac J. 2017;54:281–286. [PubMed: 27115562]
31. de Lima RL, Hoper SA, Ghassibe M, et al. Prevalence and nonrandom distribution of exonic mutations in interferon regulatory factor 6 in 307 families with Van der Woude syndrome and 37 families with popliteal pterygium syndrome. Genet Med. 2009;11:241–247. [PubMed: 19282774]
32. Fitsialos G, Chassot AA, Turchi L, et al. Transcriptional signature of epidermal keratinocytes subjected to in vitro scratch wounding reveals selective roles for ERK1/2, p38, and phosphatidylinositol 3-kinase signaling pathways. J Biol Chem. 2007;282:15090–15102. [PubMed: 17363378]
33. Turchi L, Chassot AA, Rezzonico R, et al. Dynamic characterization of the molecular events during in vitro epidermal wound healing. J Invest Dermatol. 2002;119:56–63. [PubMed: 12164925]
34. Kousa YA, Zhu H, Fakhouri WD, et al. The TFAP2AIRF6-GRHL3 genetic pathway is conserved in neurulation. Hum Mol Genet. 2019;28:1726–1737. [PubMed: 30689861]
35. Rahimov F, Marazita ML, Visel A, et al. Disruption of an AP-2alpha binding site in an IRF6 enhancer is associated with cleft lip. Nat Genet. 2008;40:1341–1347. [PubMed: 18836445]
36. Zucchero TM, Cooper ME, Maher BS, et al. Interferon regulatory factor 6 (IRF6) gene variants and the risk of isolated cleft lip or palate. N Engl J Med. 2004;351:769–780. [PubMed: 15317890]
37. Andriessen MP, Niessen FB, van de Kerkhof PC, Schalkwijk J. Hypertrophic scarring is associated with epidermal abnormalities: an immunohistochemical study. J Pathol. 1998;186:192–200. [PubMed: 9924436]
38. Usui ML, Mansbridge JN, Carter WG, Fujita M, Olerud JE. Keratinocyte migration, proliferation, and differentiation in chronic ulcers from patients with diabetes and normal wounds. J Histochem Cytochem. 2008;56:687–696. [PubMed: 18413645]
39. Biggs LC, Rhea L, Schutte BC, Dunnwald M. Interferon regulatory factor 6 is necessary, but not sufficient, for keratinocyte differentiation. J Invest Dermatol. 2012;132:50–58. [PubMed: 21918538]
40. Xu X, Han J, Ito Y, Bringas P, Urata MM, Chai Y. Cell autonomous requirement for Tgfbr2 in the disappearance of medial edge epithelium during palatal fusion. Dev Biol. 2006;297: 238–248. [PubMed: 16780827]
41. Biggs LC, Goudy SL, Dunnwald M. Palatogenesis and cutaneous repair: a two-headed coin. Dev Dyn. 2015;244:289–310. [PubMed: 25370680]
42. Nathan C, Ding A. Nonresolving inflammation. Cell. 2010;140: 871–882. [PubMed: 20303877]
43. Schonmeyr B, Wendby L, Campbell A. Early surgical complications after primary cleft lip repair: a report of 3108 consecutive cases. Cleft Palate Craniofac J. 2015;52:706–710. [PubMed: 25286156]

44. Aerts A, de Volder I, Weinberg SM, et al. Haploinsufficiency of interferon regulatory factor 6 alters brain morphology in the mouse. Am J Med Genet A. 2014;164A:655–660. [PubMed: 24357509]
45. Botti E, Spallone G, Moretti F, et al. Developmental factor IRF6 exhibits tumor suppressor activity in squamous cell carcinomas. Proc Natl Acad Sci U S A. 2011;108:13710–13715. [PubMed: 21807998]
46. Li D, Cheng P, Wang J, et al. IRF6 is directly regulated by ZEB1 and ELF3, and predicts a favorable prognosis in gastric cancer. Front Oncol. 2019;9:220. [PubMed: 31019894]
47. Nobeyama Y, Nakagawa H. Silencing of interferon regulatory factor gene 6 in melanoma. PLoS One. 2017;12:e0184444. [PubMed: 28877249]
48. Bailey CM, Kahalkahali-Ellis Z, Kondo S, et al. Mammary serine protease inhibitor (Maspin) binds directly to interferon regulatory factor 6. Identification of a novel serpin partnership. J Biol Chem. 2005;280:34210–34217. [PubMed: 16049006]
49. Michel M, Smith LT, Fleckman P, Dale BA. The calcium activated neutral protease calpain I is present in normal fetal skin and is decreased in neonatal harlequin ichthyosis. Br J Dermatol. 1999;141:1017–1026. [PubMed: 10606846]
50. Hager B, Bickenbach JR, Fleckman P. Long term culture of murine epidermal keratinocytes. J Invest Dermatol. 1999;112:971–976. [PubMed: 10383747]
51. Dunnwald M, Chinnathambi S, Alexandrunas D, Bickenbach JR. Mouse epidermal stem cells proceed through the cell cycle. J Cell Physiol. 2003;195:194–201. [PubMed: 12652646]
52. Michel M, Török N, Godbout M-J, et al. Keratin 19 as a biochemical marker of skin stem cells in vivo and in vitro: keratin 19 expressing cells are differentially localized in function of anatomic sites, and their number varies with donor age and culture stage. J Cell Sci. 1996;109:1017–1028. [PubMed: 8743949]
53. Germain L, Guignard R, Rouhabia M, Auger FA. Early basement membrane formation following the grafting of cultured epidermal sheets detached with thermolysin or Dispase. Burns. 1995;21:175–180. [PubMed: 7794497]

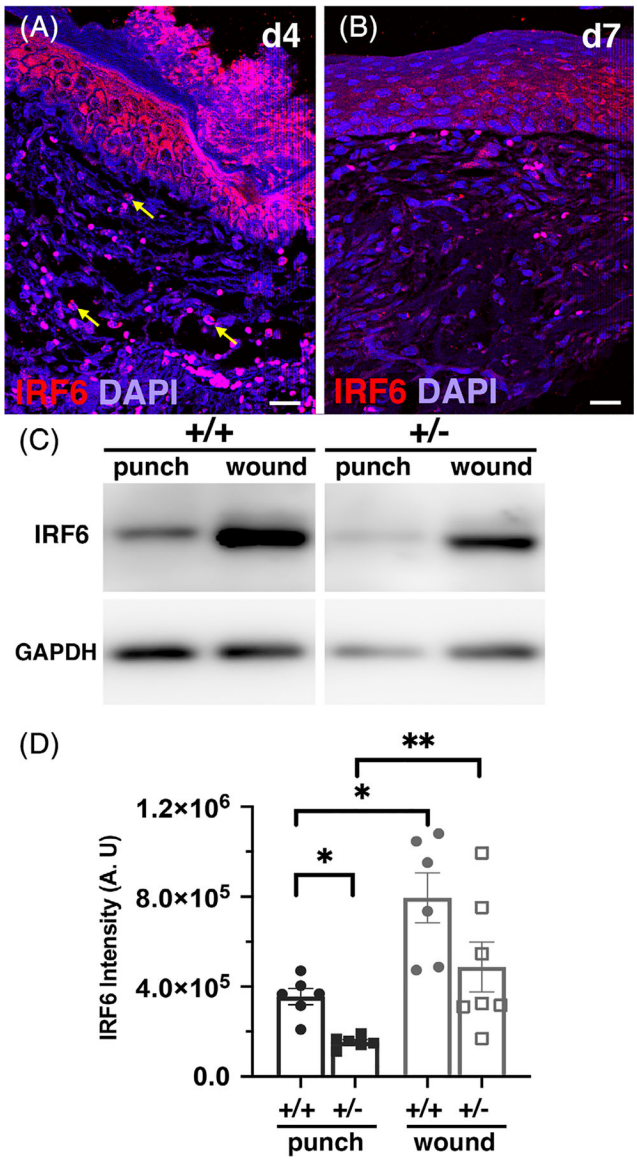

FIGURE 1.

Irf6 is reduced in heterozygous mice, and elevated in wounds. A and B, Immunofluorescent staining for Irf6 (red) and DAPI (blue) of 4-day (A) and 7-day (B) wild-type wound paraffin sections. Yellow arrows point to innate immune cells. C, Western blot for Irf6 and GADPH (one representative of three experiments, images collated from the same gel) of unwounded and wounded RIPA tissue extracts from wild-type and heterozygous animals. D, Quantification of Irf6 protein levels as determined by Western blot analysis. Data show the means (N = 6–7 per groups) ± SEM, *$P < .05$ and **$P < .01$ after Kruskal-Wallis test. DAPI, 4',6-diamidino-2-phenylindole; RIPA, radioimmunoprecipitation assay

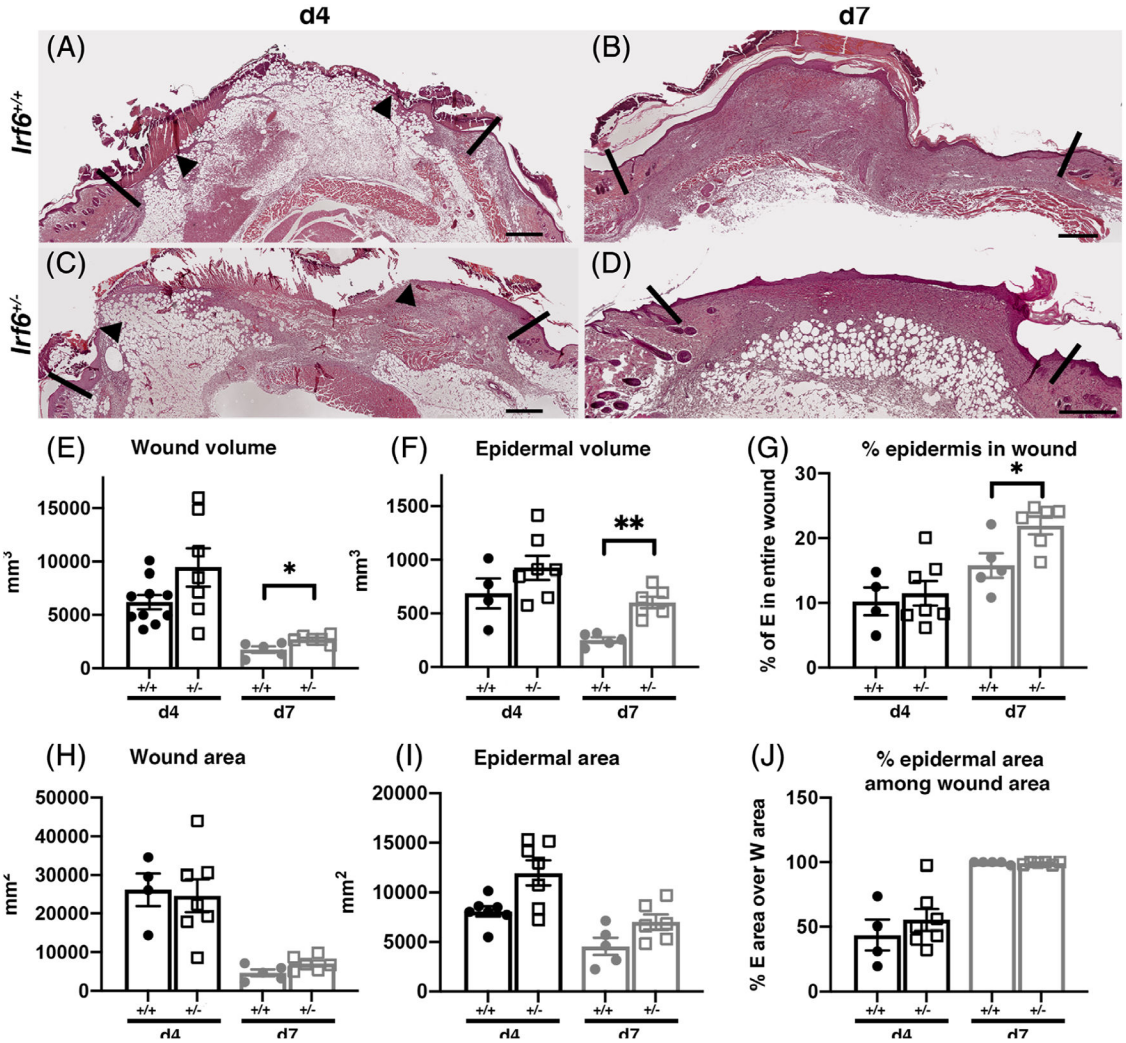

FIGURE 2.

Altered wound healing in mice with reduced levels of Irf6. A-D, Representative histological features of 4-day (A, C) and 7-day (B, D) wound sections chosen in the middle of *Irf6*$^{+/+}$ (A, B) and *Irf6*$^{+/-}$ (C, D) wounds. Scale bar = 500 μm; arrow head indicates the epithelial wound margin and the vertical black lines the limit between unwounded and wounded tissue. E-J, Computed morphometric measurements of 4- and 7-day wounds. E, F, H, and I are directly measured on the wound as previously described.[22] G, Percentage of epidermis is calculated by dividing the epidermal volume by the wound volume. J, Percentage of epidermal area among wound area is calculated by dividing the epidermal area by the wound area. Data show the means (N = 4–7 per groups) ± SEM, **P* < .05 and ***P* < .01 after Mann-Whitney test

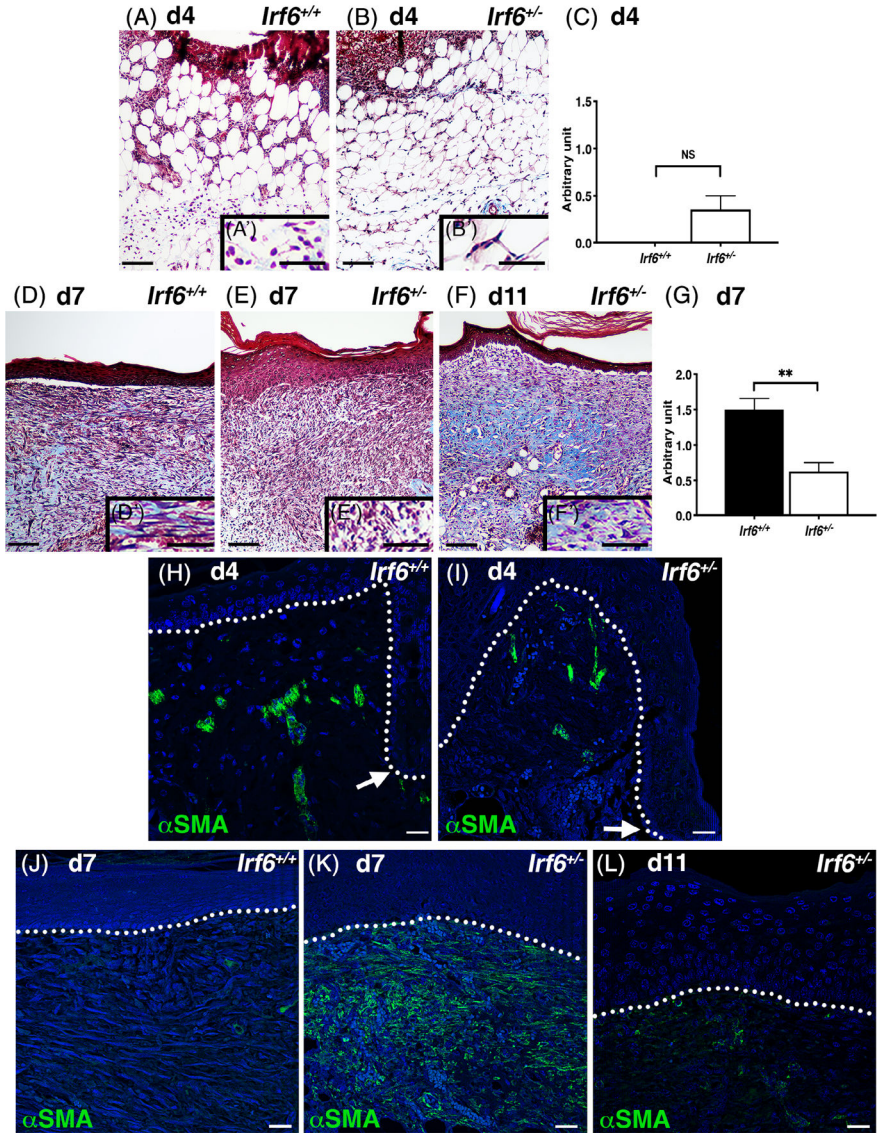

FIGURE 3.

Irf6 is required for the maturation of the granulation tissue. A, B, D, E, and F, Masson's Trichrome histological staining of wild-type (A, D) and *Irf6*$^{+/-}$ (B, E, F) 4-day (A, B), 7-day (D, E), and 11-day (F) wounds. Images represent a section of the middle of the wound. A', B', D', E', and F' are magnified regions of (A), (B), (D), (E), and (F), respectively, immediately below the epidermis. Scale bars = 100 and 50 μm for inserts. C and G, Quantification of collagen deposition in 4-day (C) and 7-day (G) wounds as evaluated by arbitrary scale (0–3). Data show the means (N = 4–7 per groups) ± SEM, NS = non significant, $^{**}P < .005$ after Student *t* test. H-L, Immunofluorescent staining for α-smooth muscle actin (α-SMA, green) and DAPI (blue) of wild-type (H, J) and *Irf6*$^{+/-}$ (I, K, L) 4-day (H, I), 7-day (J, K), and 11-day (L) wounds. White arrows point to the leading edge (H-I) and dotted lines indicate the basement membrane (H-L). Scale bars = 25 μm. DAPI, 4',6-diamidino-2-phenylindole

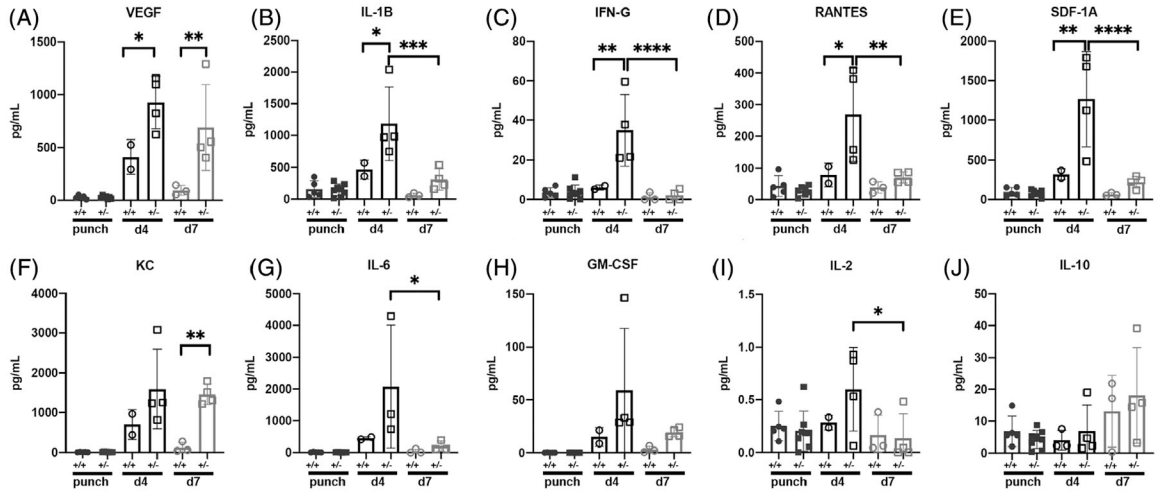

FIGURE 4.

Irf6 represses inflammatory cytokines during tissue repair. Cytokine (IL1-B, B; IFN-g, C; RANTES, D; KC, F; IL-6, G; IL-2, I; IL-10, J) and growth factors (VEGF, A; SDF-1A, E; GM-CSF, H) in wild-type and *Irf6*$^{+/-}$ punches (unwounded skin) and 4- and 7-day wounds as determined by Luminex assay. Data show the means (N = 2–7 per groups) ± SEM, **P* < .05, ***P* < .01, ****P* < .005, *****P* < .0001 after Mann-Whitney test

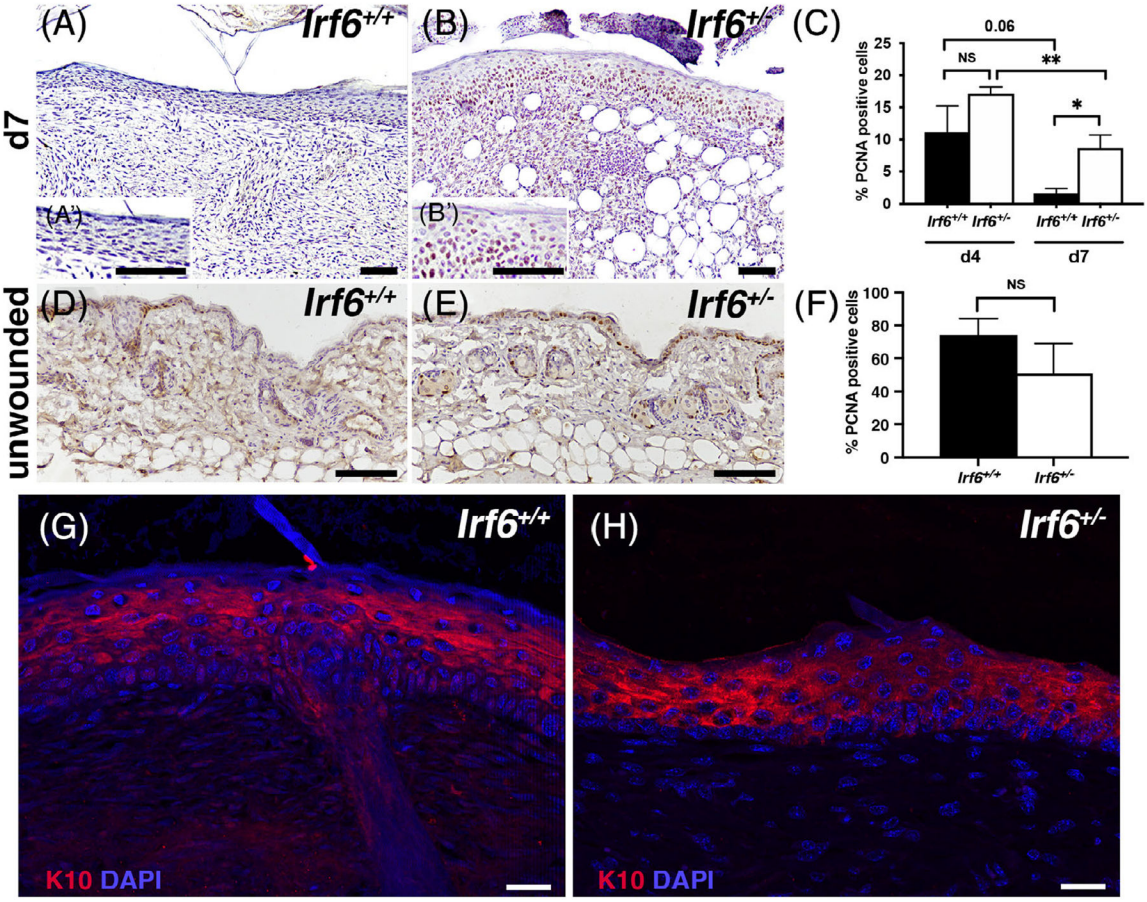

FIGURE 5.

Reduced Irf6 levels increase epidermal proliferation in neoformed epidermis in vivo. A, B, D, and E, Immunohistochemical staining for PCNA (brown) counter stained with hematoxylin (blue) of wild-type (A, D) and *Irf6*$^{+/-}$ (B, E) 7-day wounds (A, B) and unwounded adult back skin (D, E). Images in (A) and (B) represent a section of the middle of the wound. A' and B' are magnified regions of (A) and (B). C, Percentage of basal cells positive for PCNA in the migrating tongue (4-day wounds) or neoformed epidermis (7-day wounds). F, Percentage of basal cells positive for PCNA in unwounded adult back skin. Data show the means (N = 4–7 per groups) ± SEM, **P* < .05, ***P* < .005, NS = nonsignificant after Student *t* test. Scale bars = 100 μm. G and H, Immunofluorescent staining for keratin 10 (K10, red) and DAPI (blue) of wild-type (G) and *Irf6*$^{+/-}$ (H) unwounded skin flanking 7-day wounds. Scale bars = 25 μm. PCNA, proliferating cell nuclear antigen

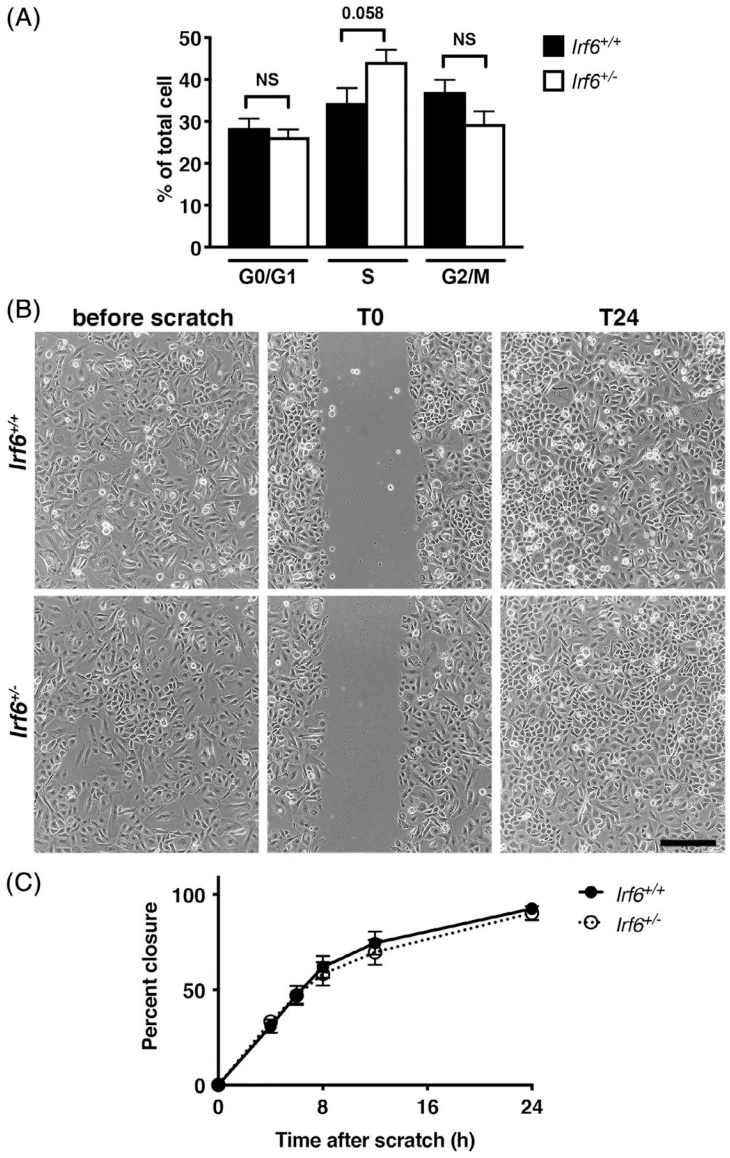

FIGURE 6.

Cell proliferation and migration is not affected by Irf6 levels in murine keratinocytes. A, Cell cycle profile of wild-type and *Irf6*$^{+/-}$ murine keratinocyte as determine by FACScan after being resuspended in propidium iodide. The percentage of cells in each phase of the cell cycle was determined based upon their DNA content (cells with 2n = G0/G1; cells with >2n and <4n = S; cells with 4n = G2/M). B, Phase contrast micrographs of in vitro scratch wounds in confluent monolayers of wild type and *Irf6*$^{+/-}$ murine keratinocytes. Cells were grown to confluency then scratched with a yellow tip (T0). By 24 hours (T24), both groups of keratinocytes had closed the scratch. Scale bar = 100 μm. C, Quantification of the percentage of wound closure over time. Data show the means ± SEM. NS = nonsignificant after Student *t* test. N = 10 to 14 per groups

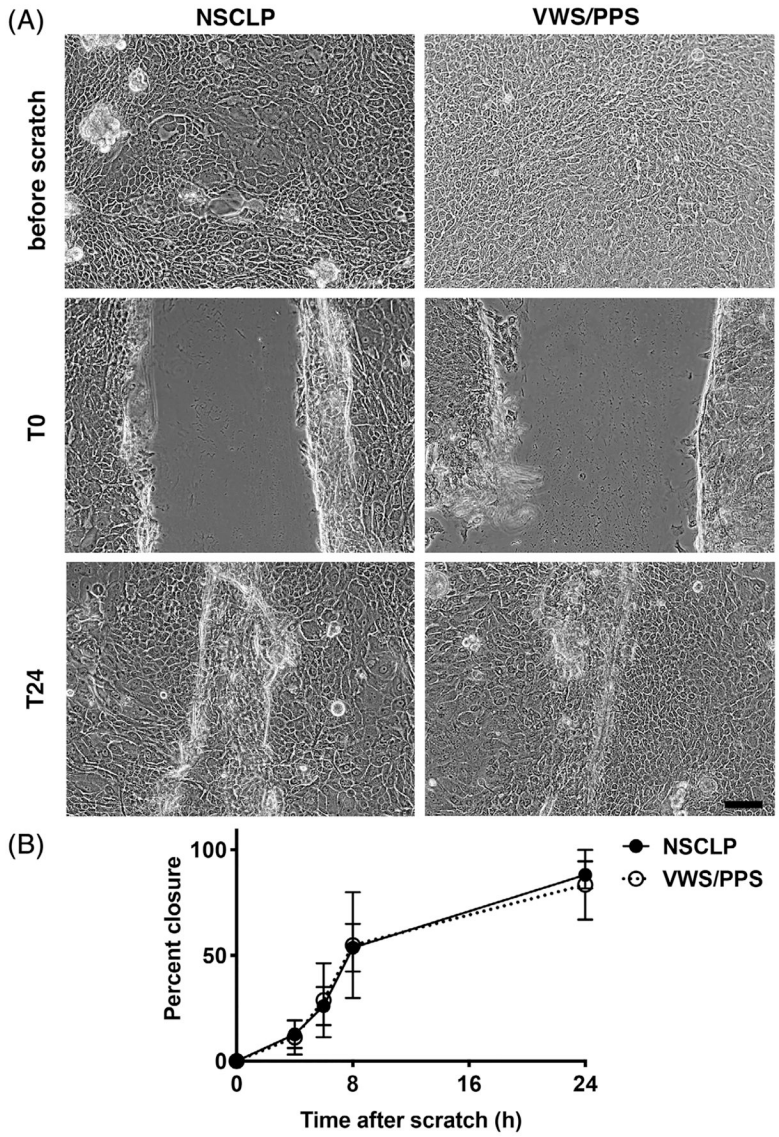

FIGURE 7.

Keratinocytes from patients with *IRF6* mutations properly close an in vitro scratch wound. A, Phase contrast micrographs of in vitro scratch wounds in confluent monolayers of human keratinocytes from individuals with nonsyndromic cleft lip and palate (NSCLP) or with an *IRF6* mutation leading to Van der Woude or popliteal pterygium syndromes (VWS/PPS). Cells were grown to confluency (before scratch) then scratched with a yellow tip (T0). By 24 hours (T24), both groups of keratinocytes had closed the scratch. Scale bar = 100 μm. B, Quantification of the percentage of wound closure over time. Data show the means ± SEM. N = 9 for NSCLP, N = 3 for VWS/PPS (see Table 1 for details)

TABLE 1

Characteristics of included children with cleft lip and palate

Individual[a]	Cleft type	Lip pits	IRF6 mutation	Genotype at rs642961	Genotype at rs2235371
1[b]	BCL+A	Yes	R250Q[31]	GG	GG
2	UCL+A	Yes	R412X[31]	nd	GA
3	UCLP+A	No		GG	nd
4	CLP	No		GG	GG
5	BCLP+A	No		GG	GG
6	UCLP	No		GG	GA
7	BCLP+A	No		GG	GG
8	BCLP+A	No		GG	nd
9	UCLP+A	No		GG	GG
10	UCLP	Yes	R84C	GG	GG
11	UCLP	No		nd	nd
12	UCLP	No		nd	nd

Abbreviations: A, alveolus; B, bilateral; CL, cleft lip only; CLP, cleft lip/palate; nd, not determined; U, unilateral.

[a] Individual 1 to 9 are the same as Hixon et al.[30]

[b] This child is the same as individual # 14 in our previous study.[20]